Supplementary Information

Impact of chirality in the amorphous state of conglomerate forming system: case study of N-acetyl-α-methylbenzylamine

Bienvenu Atawa †§T*, Nicolas Couvrat §, Frédéric Affouard‡, Natália T. Correia‡,

Gérard Coquerel §, Allisson Saiter-Fourcin †

† Normandie Univ, UNIROUEN, INSA Rouen, CNRS, GPM, 76000 Rouen, France

§ Normandie Univ, UNIROUEN, SMS, 76000 Rouen, France

‡ Univ Lille, CNRS, INRA, ENSCL, UMR 8207, UMET, Unité Matériaux et Transformations, F59000 Lille, France

ᵀ Univ-Lyon, Université Lyon 1, Ingénierie des Matériaux Polymères, CNRS UMR 5223, 69622 Villeurbanne, France

A) Thermal properties of amorphous Nac-MBA

Amorphous Nac-MBA was obtained at various ee by melt cooling at 70 K/min. This cooling permitted to amorphize all the analyzed compositions (0≤ ee ≤ 75%). The samples were then submitted to a heat only temperature modulation protocol with a heating rate of 2K/min, modulation amplitude of ± 0.318 K and a period of 60 s. Figure S1 depicts the glass transition signature upon heating at variable ee.

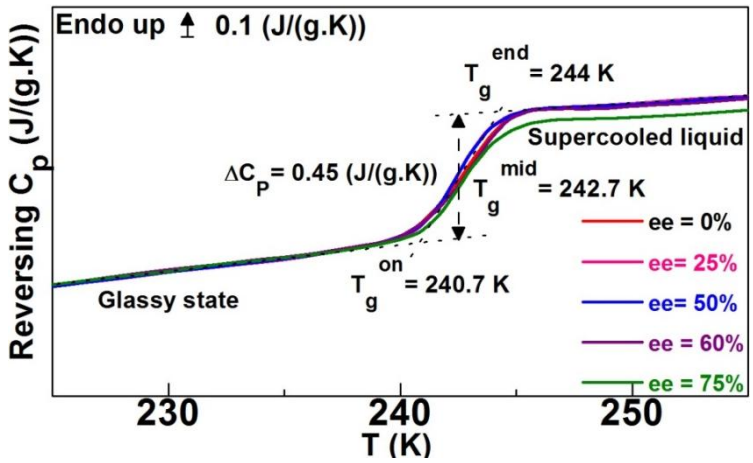

Figure S1: Reversing specific heat capacity as a function of temperature at a heating rate of 2 K/min, oscillation amplitude of ± 0.318 K and a period of 60 s for several ee.

The glass transition temperature (T_g^{on} = 240.7 K) is independent of the ee. The heat capacity jump at T_g ΔC_P is equal to 0.45± 0.01 (J/(g.K)) for ee ≤ 60%, and decreases slightly to down to 0.42± 0.01 (J/(g.K)) for ee = 75%. Even though the melting temperature may differ for more than 25°C between the pure enantiomer and the racemic composition, the Tg of both samples is the same. In chiral systems it is generally observed that Tg is independent of the composition in accordance to the Gordon Taylor law. This behavior has been reported for many different chiral systems such as ibuprofen [1], diprophylline [2], limonene[3] and independently of their crystalline typology. This result may suggest that Tg remains insensitive to the handedness of the system but governed by the backbone of the model molecule. The slight difference observed in the heat capacity may indicate that at ee=75%, Nac-MBA may possess less degree of freedom (lower configurational entropy) considering the higher crystallization propensity in comparison to lower ee.

B) Molecular mobility of amorphous Nac-MBA

Figure S2 depicts the frequency dependency of the dielectric loss at several ee below Tg. Independently of the ee, two secondary processes appear. The dielectric loss peak of all the samples seems similar even though they do not superimpose perfectly. The nature of both processes has been discussed in our previous work for an ee= 50% [4]. It is improbable that the ee intrinsically modifies the microscopic origin of these secondary processes since both enantiomers possess identical flexible branches and the same molecular unit but of opposite chirality.

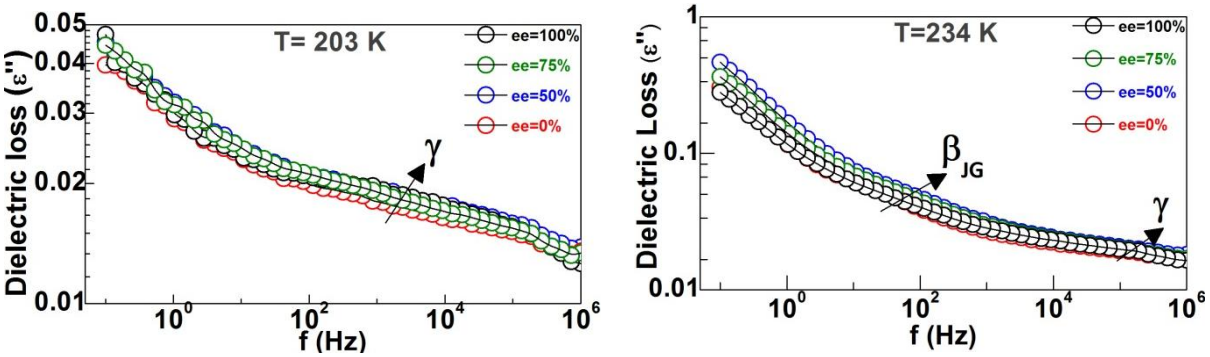

Figure S2: Frequency dependency of the dielectric loss at various ee in the glassy state a) T = 203 K, b) T = 234 K.

The frequency evolution of the dielectric loss peak at several temperatures in the supercooled liquid (250 K and 259 K) and liquid state (313 K and 383 K) are reported (for different ee) in figure S3.

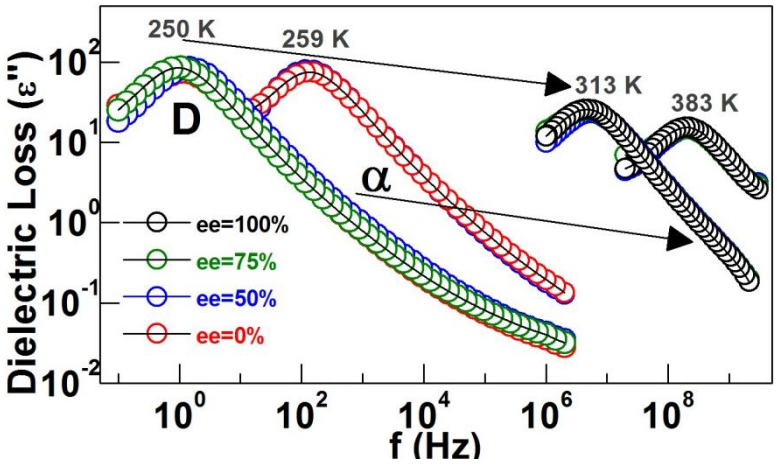

Figure S3: Isothermal frequency evolution of the dielectric loss in the supercooled liquid state for different ee and temperatures (250 K, 259 K, 313 K and 383 K)

The very intense and slow single exponential Debye (D) response localized at the lowest frequency range overlaps with the structural relaxation α. The different samples (ee= 100%, ee= 75% and ee= 0%) illustrate identical relaxation processes as those reported for ee= 50%. Thus, the relaxational landscape seems not to be impacted by chirality in the case of Nac-MBA.

In order to subtract the essential information about these relaxation processes (relaxation time, shape parameters, dielectric strength) the isothermal dielectric loss peak was fitted with a sum of Havriliak-Negami model functions and a conductivity contribution when necessary (see Eq S1).

$$\varepsilon^*(\omega) = \varepsilon'(\omega) - i\varepsilon''(\omega) = \sum_k^n \left[\frac{\Delta\varepsilon_k}{\left(1+i\left(\omega\tau_{HN_k}\right)^{\alpha_{HN_k}}\right)^{\beta_{HN_k}}} + \varepsilon_{\infty_k} \right] + -i\left(\frac{\sigma_0}{\varepsilon_0\omega}\right)^N \qquad \text{Eq S1}$$

where σ_0 is the specific dc-conductivity; ε_0 the permittivity of the vacuum ($\varepsilon_0 = 8.854 \times 10^{-12} F/m$); $\omega = 2\pi f$ the angular frequency; N gives the exponent of the frequency dependence of ε''; k sums over the different relaxation processes, τ_{HN} is a characteristic relaxation time regards to the frequency of maximal loss f_{max}; $\Delta\varepsilon$ is the dielectric relaxation strength of the process under investigation; ε_∞ the high frequency limit of the real permittivity $\varepsilon'(\omega)$. α_{HN} and β_{HN} are fractional shape parameters which detail the symmetric and asymmetric broadening of the complex dielectric response in such a way that $0 < \alpha_{HN}, \alpha_{HN}.\beta_{HN} \leq 1$ [5]. From τ_{HN}, α_{HN} and β_{HN} the time scale τ of each relaxation process is given by:

$$\tau = \frac{1}{2\pi f_{max}} = \tau_{HN}\left[\sin\left(\frac{\alpha_{HN}\pi}{2+2\beta_{HN}}\right)\right]^{\frac{-1}{\alpha_{HN}}}\left[sin\left(\frac{\alpha_{HN}\beta_{HN}\pi}{2+2\beta_{HN}}\right)\right]^{\frac{1}{\alpha_{HN}}} \qquad \text{Eq S2}$$

The fitting procedure in the present case is somehow challenging since the slow Debye and structural relaxation processes overlap. Additionally, the secondary processes are of low magnitude and poorly

resolved. Thus, the shape parameters and their temperature dependencies may be summited to high uncertainty and must be taken as indicative values. The shape parameters of the four processes are displayed in table S1.

Table S1: Shape parameters of the four processes for variable ee.

	ee = 0%		ee = 50%		ee = 75%		ee = 100%	
	α_{HN}	β_{H}	α_{HN}	β_{HN}	α_{HN}	β_{H}	α_{HN}	β_{HN}
D	0.96	1	0.95 - 1	1	0.95 - 1	1	0.95 - 1	1
α	0.6	1	0.58 - 0.6	1	0.6	1	0.6	1
β_{JG}	0.4 - 0.5	1	0.38 - 0.45	1	0.42 - 0.45	1	0.4 - 0.45	1
γ	0.11 - 0.15	1	0.14	1	0.14	1	0.14	1

Globally the symmetric and asymmetric broadening are typically the same and independent of the enantiomeric composition. The temperature dependence of the relaxation time of both secondary processes was fitted with an Arrhenius function illustrated in equation Eq S3 and expressed as follow:

$$\tau\,(T) = \tau_{\infty} \exp\left(\frac{E_A}{RT}\right) \qquad \text{Eq S3}$$

where τ_{∞} is the pre-exponential factor, E_A the activation barrier energy and *R* the ideal gas constant. Table S2 sums up the fitting parameters derived from the Arrhenius equation.

Table S2: Fitting parameters of the Arrhenius function used to describe the temperature evolution of the relaxation time of γ, β at several ee. Each color is associated to a given enantiomeric composition: ee= 100% (black) ee= 75% (green) ee= 50% (blue) and ee= 0% (red).

$T < T_g$	$E_a\ (kJ.mol^{-1})$	τ_{∞}(s)
γ- process	38 ± 2	$(1.4 \pm 1.0) \times 10^{-13}$
β-process	70 ± 10	$(2.38 \pm 2.37) \times 10^{-15}$
γ - process	39 ± 2	$(9 \pm 7) \times 10^{-14}$
β-process	73 ± 8	$(5.48 \pm 5.47) \times 10^{-17}$
γ - process	39 ± 2	$(7 \pm 5) \times 10^{-14}$
β -process	72 ± 8	$(5.37 \pm 5.36) \times 10^{-17}$
γ - process	36 ± 2	$(6 \pm 4) \times 10^{-13}$
β -process	83 ± 9	$(6.71 \pm 6.70) \times 10^{-19}$

The fitting parameters of the relaxation time temperature dependence indicate that the secondary γ- process is insensitive to chirality since the activation energy E_a and the high temperature limit of the relaxation time τ_∞ are not ee dependent. Thus, secondary γ- process expressed the same microscopic origin independently of chirality.

As mentioned in our previous paper for ee= 50% [4], secondary β process is of β_{JG} type. This behavior is not affected by the enantiomer ratio. The activation energy of β_{JG} process when ee= 0% seems to deviate from the average value presented at other ee. Furthermore, τ_∞ values are typically higher than the value usually obtained in glass forming liquids (approximately $10^{-14}s - 10^{-13}s$). At our understanding such differences are not related to any physical meaning but may be inherent to the fitting procedure, since for this specific process the fitting was conducted with few data. Nevertheless these analyses may suggest that localized motions seem to be ee independent.

The temperature dependence of the relaxation time of both α and D processes were fitted with the VFTH empirical function displayed in Eq S4:

$$\tau(T) = \tau_\infty \exp\left(\frac{B}{T - T_0}\right) \qquad \text{Eq S4}$$

where τ_∞ is the high temperature limit relaxation time, B an empirical parameter representative of the deviation from linearity and T_0 the Vogel temperature. Table S3 illustrates the fitting parameters of the both α and D relaxation time temperature dependences derived from the VFTH equation.

Table S3: Fitting parameters of the VFTH function used to describe the temperature evolution of the relaxation time of both α and D processes at ee= 50% (blue) and ee= 0% (red).

$T > T_g$	B (K)	τ_∞(s)	T_0(K)
α-process VFTH	1230 ± 56	$(3 \pm 1) \times 10^{-14}$	205 ± 1
D- process VFTH	1074 ± 25	$(14 \pm 3) \times 10^{-13}$	207 ± 1
α-process VFTH	1081 ± 23	$(9 \pm 6) \times 10^{-14}$	209 ± 2
D-process VFTH	957 ± 95	$(27 \pm 3) \times 10^{-13}$	211 ± 1

Since the samples at high ee (ee > 50%) strongly crystallize in the supercooled-liquid state very few reliable data could be collected regarding the molecular mobility of both D and α relaxation processes. Consequently, the fitting procedure of the relaxation time temperature dependence is achieved for samples at ee ≤ 50%. The VFTH fitting parameters of the D and α relaxation time temperature dependence as function of the ee suggest similar dynamics. In the case of α process the Vogel temperature T_0 increases for approximately 4.4 K when changing the composition from ee = 50% down to ee = 0%. This difference is nearly the same for D-process (4K). Additionally, the glass

transition temperature T_g is not perfectly the same regarding the two compositions. The difference T_g (ee = 0%) - T_g (ee = 50%) = 0.8 K is very small and thus not significant. These results may suggest that the relaxation rate at ee = 50% seems very similar to that of ee = 0%. The same conclusion can be drawn for higher ee considering the high temperature domain since the relaxation time coincides for all the ee.

The calculated fragilities of both samples are in the same range, m= 119 ± 10 for ee = 0% and m = 108 ± 5 for ee = 50%. The fragility parameter is used to quantify the deviation of the structural relaxation time from the Arrhenius behavior and given by Eq S5:

$$m = \frac{BT_g}{\ln 10\left(T_g - T_0\right)^2} \qquad \text{Eq S5}$$

This result allows classifying Nac-MBA as a fragile system independently of it enantiomeric composition. Thus, the cooperative motions associated to the glass dynamic and the transient motions of linear H-bond aggregates associated to the D relaxation are insensitive to chirality.

References

1 M. T. O. Abe, M. T. Viciosa, N. T. Correia and F. Affouard, Impact of chirality on peculiar ibuprofen molecular dynamics: hydrogen bonding organization and syn vs. anti carboxylic group conformations, *Phys. Chem. Chem. Phys.*, 2018, **20**, 29528–29538.

2 Q. Viel, C. Brandel, Y. Cartigny, M. E. S. Eusébio, J. Canotilho, V. Dupray, E. Dargent, G. Coquerel and S. Petit, Crystallization from the Amorphous State of a Pharmaceutical Compound: Impact of Chirality and Chemical Purity, *Cryst. Growth Des.*, 2017, **17**, 337–346.

3 H. E. Gallis, J. C. van Miltenburg and H. A. J. Oonk, Polymorphism of mixtures of enantiomers: A thermodynamic study of mixtures of D- and L-limonene, *Phys. Chem. Chem. Phys.*, 2000, **2**, 5619–5623.

4 B. Atawa, N. T. Correia, N. Couvrat, F. Affouard, G. Coquerel, E. Dargent and A. Saiter, Molecular mobility of amorphous N-acetyl-α-methylbenzylamine and Debye relaxation evidenced by dielectric relaxation spectroscopy and molecular dynamics simulations, *Phys. Chem. Chem. Phys.*, 2019, **21**, 702–717.

5 F. Kremer and A. Schönhals, Eds., *Broadband Dielectric Spectroscopy*, Springer-Verlag, Berlin Heidelberg, 2003.